Carboxylate Coated Nickel Ferrite Nanoparticles for High-gradient Magnetic Separation

T.M. Trad[1], R. Alvarez[1], A. Apblett[2] and K.S. Martirosyan[3]

[1]Department of Chemistry and Environmental Sciences, University of Texas at Brownsville, Brownsville, TX, USA, 78520, tarek.trad@utb.edu
[2]Department of Chemistry, Oklahoma State University, Stillwater, OK, USA 74078
[3]Department of Physics and Astronomy, University of Texas at Brownsville, Brownsville, TX, USA, 78520, karen.martirosyan@utb.edu

ABSTRACT

Magnetic separation is a complex physical process in which magnetically susceptible composites are extracted from a liquid mixture using the magnetic properties of the composite. Several separation procedures are developed based on magnetic susceptibility, magnetohydrostatic, magnetohydrodynamic, and separation using eddy currents. The principle of separation by magnetic susceptibility consists of different actions of the magnetic force in competition with drag, gravity or friction forces. High-gradient magnetic separation (HGMS) is a process that utilizes magnetic susceptibility to effectively separate magnetic materials from a nonmagnetic liquid medium. Applications of HGMS include kaolin clay purification, removal of iron particles from process streams in steel and power plants, desulphurization of coal, wastewater treatment of bacteria, organic substances and microorganisms through magnetic seeding. In the present report, we describe a new nonhydrolytic single precursor route for the synthesis of carboxylate coated nickel ferrite nanoparticles to separate soluble pentavalent arsenic As(V) from water. Using nonhydrolytic techniques holds great potential for producing superparamagnetic metal oxide nanoparticles with superior properties related to surface composition and defect structure.

Keywords: Magnetic separation, carboxylate coating, nickel ferrite, superparamagnetic nanoparticles, arsenic contamination

1 INTRODUCTION

Serious concerns have been raised in many regions of the globe regarding arsenic (As) contamination in water [1]. Arsenic's ingestion in drinking water can cause many health problems such as bladder, kidney, and skin cancers, muscular weakness, nerve tissue injuries, and blackfoot disease [2,3]. Millions of people worldwide have been reported to be at risk due to arsenic intake from natural waters [4]. Considering arsenic's high toxicity and deleterious effect on human health, the World Health Organization (WHO) have shown a more stringent attitude towards the standard for arsenic in drinking water by recommending the 10 μg/l as maximum contaminant level (MCL) of arsenic in 1993. After reviewing the science and economics behind implementing the new standard set by the WHO, the US Environmental Protection Agency (EPA) decided to lower the MCL of arsenic from 50 to 10 μg/l starting January 2006 [5]. As a result of this new measure, effective and competitive technologies for arsenic remediation are needed in order to meet EPA's recent requirement.

In nature, arsenic occurs in a variety of mineral forms of which a large proportion is present as arsenates and the remaining percentage includes arsenites, arsenides, sulfides, sulfosalts, oxides, silicates, and elemental arsenic. In aqueous aerobic environments, inorganic arsenic is predominantly found in its thermodynamically stable pentavalent forms (H_3AsO_4, $H_2AsO_4^{-1}$, $HAsO_4^{-2}$ and AsO_4^{-3}), whereas, trivalent arsenite (H_3AsO_3, and $H_2AsO_3^-$) is more prevalent under reducing conditions such as anaerobic groundwaters [6]. Methyl and dimethyl arsenic acids are organic forms of arsenic which may also be found in natural waters as an outcome of application of organo-arsenical pesticides, and via biomethylation mechanisms of microorganisms. Conventional techniques available for the removal of arsenic from contaminated water are: (i) coagulation/precipitation, (ii) lime softening, (iii) adsorption, (iv) ion exchange, (v) membrane filtration, and electrodialysis [7]. These physico-chemical methods are primarily effective for As(V) remediation. However, certain limitations are associated with the use of these treatment techniques. Among the limiting factors responsible for low efficiency are operation and equipment cost, competitive interference of ions on removal performance, need for post treatment steps, use and handling of chemicals, and production of large quantities of high arsenic content sludge. Recently, High Gradient Magnetic Separation (HGMS) technology was proven to separate nanoparticles with average particle diameters as low as 2 nm [8]. In this study, nonhydrolytic single precursor route for the synthesis of capped nickel ferrite nanoparticles is described. These novel magnetic nanoparticles were investigated for their ability to adsorb pentavalent arsenic from water. After the adsorption process, these materials were easily recovered using a lab scale magnetic filter.

2 EXPERIMENTAL DETAILS

Using nonhydrolytic techniques holds great potential for producing metal oxide nanoparticles with superior properties related to surface composition and defect structure [9]. Advantages resulting from nonhydroxylated surfaces may be of interest in cataylsis, ceramics, magnetic data storage, and environmental applications. For all precursor synthesis reactions, reagents were of analytical grade and used as received. The chemicals used were as follows; iron(III) chloride hexahydrate [$FeCl_3.6H_2O$, Aldrich]; iron(III) nitrate nonahydrate [$Fe(NO_3)_3.9H_2O$, Aldrich]; nickel(II) chloride hexahydrate [$NiCl_2.6H_2O$, Aldrich]; octanoic acid [$C_8H_{16}O_2$, Eastman]; stearic acid [$C_{18}H_{36}O_2$, Aldrich]; ammonium hydroxide [NH_4OH]; 1,2,3,4-Tetrahydronaphthalene (tetralin) [$C_{10}H_{12}$, Fluka].

The magnetic nanoparticles and their precursors were characterized using several techniques. Powder X-ray diffraction (XRD) patterns were recorded on a Bruker AXS D8 Advance diffractometer using Cu Kα radiation. The peaks were profiled with a Pearson 7 model using Topas P software. Infrared spectroscopic measurements were performed on a Nicolet Magna-IR 750 spectrometer. Approximately 10 mg of the precursor or the capped magnetic nanoparticles was added to a 100 mg FTIR-grade potassium bromide and mixed thoroughly. The blend was then finely ground and spectra in the 4000–400 cm^{-1} region were collected by diffuse reflectance of the ground powder. Typically, 128 scans were recorded and averaged for each sample (4.0 cm^{-1} resolution) and the background was automatically subtracted. Transmission electron micrographs (TEM) were obtained using a JEOL JEM-100CXII electron microscope. For this purpose a 0.1 % w/v stable dispersions of the nanoparticles in toluene were prepared. A drop of each of the powder dispersions was carefully placed on a copper grid surface and dried before micrographs were generated. Dynamic light scattering (DLS) measurements were performed on the capped magnetite and nickel ferrite nanoparticles suspensions with a Malvern HPPS 3001 instrument. Particle size measurements were obtained at 25.0 °C with dispersant viscosity and refractive index values of 0.55 cP and 1.491 respectively. The magnetic properties of the samples were measured at room temperature using a vibrating sample magnetometer VSM (Lake Shore Cryotronics, Inc. Model 7300) with an applied field up to 10^4 Oe.

3 SYNTHESIS OF THE CAPPED NICKEL FERRITE NANOPARTICLES

3.1. Ni-Fe(octanoate) precursor: 10.80 g of $FeCl_3.6H_2O$ were dissolved in 20 ml of ethanol. Another solution was made by dissolving 19.00 g of $NiCl_2.6H_2O$ in 30 ml of ethanol and then gradually added to the Fe^{3+} solution. A sample of 14.40 g of caprylic acid in 40.00 ml ethanol was stirred to dissolution, and a colorless solution had formed. The caprylic acid solution was then added to the stirred Fe^{3+}/Ni^{2+} solution and a dark green solution was observed. Upon the addition of 10 ml of concentrated ammonia, a light brown precipitate was formed. With a large amount of hot ethanol, the precipitate was washed to remove all the residual unreacted starting materials. Finally, after filtration, the light brown powder was dried under vacuum for 24 hours. The reaction yielded 23.79 g.

3.2. Ni-Fe(stearate) precursor: The method used for preparing the Ni-Fe(octanoate) sample was adopted for this bimetallic stearate precursor. An Fe^{3+} solution made by dissolving 5.50 g of $FeCl_3.6H_2O$ in 10 ml of ethanol. 9.60 g of $NiCl_2.6H_2O$ were dissolved in 15 ml of commercial ethanol, and the Fe^{3+} solution was added to this Ni^{2+} solution and the mixture was stirred at room temperature. A sample of 5.6 g of stearic acid was dissolved in 80 ml of ethanol and the solution was added drop-wise to the stirred mixture of iron(III) and nickel(II) solutions. Upon that addition a brown precipitate was formed immediately. The precipitate was filtered and washed with enough hot ethanol to remove all unreacted excess of starting reactants. Finally, the brown precipitate was dried under vacuum for 24 hours. The reaction yield was 11.24 g.

3.3. Synthesis of Octanoate capped nickel ferrite nanoparticles: A sample of 3.00 g of Ni-Fe(octanoate) starting material was suspended in a 100 ml of tetralin. The suspension was degassed under vacuum for 1 hour and then purged with helium for 30 minutes. The reaction vessel was then placed in a tube furnace and the temperature was set at 210 °C for 12 hours. At room temperature the light brown suspension transformed to a dark brown stable dispersion (stable for more than a year) indicating the formation of nickel ferrite nanoparticles. Adding an excess volume of acetone (300 ml), the capped nickel ferrite nanoparticles were precipitated as brown powder, which was dried under air. The solid produced was magnetic in nature. The reaction yielded 1.43 g.

3.4. Synthesis of Stearate capped nickel ferrite nanoparticles: Similarly, this sample was prepared using 2.00 g of Ni-Fe(stearate) precursor suspended in 80 ml of tetralin. Conditions mentioned in the preparation of the previous nickel ferrite nanoparticles were used in this procedure. The yield of this reaction was 1.03 g.

4 RESULTS AND DISCUSSION

The XRD diffractogram of the as-synthesized $NiFe_2O_4$(octanoate) nanoparticles is presented in Figure 1. The absence of sharp diffraction patterns characteristic of crystalline phases revealed the amorphous nature of the precursor. On the other hand many sharp and strong crystalline peaks were observed in the diffraction pattern of the resultant nanoparticles attributed to the formation of the

face-centered cubic $NiFe_2O_4$ phase. A crystallite size of 2.2 Å was determined using the Warren-Averbach method.

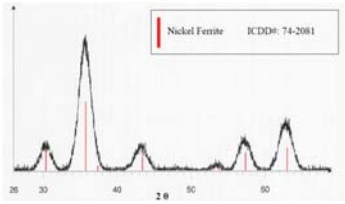

Figure 1: XRD pattern of octanoate capped nickel ferrite nanoparticles.

Infrared spectroscopic measurements were used to confirm the presence of the capping agents on the surface of nickel ferrite nanoparticles. IR spectra of the nickel-iron(octanoate) precursor and its' corresponding capped nickel ferrite nanoparticles in the region 4000 – 500 cm^{-1} are presented in Figure 2. Absorption bands below 2956 cm^{-1} indicate that the aliphatic sheath remained around the nickel ferrite, while characteristic Fe–O stretching modes in $NiFe_2O_4$ phase were associated with absorptions found at ~612 cm^{-1} [10] .

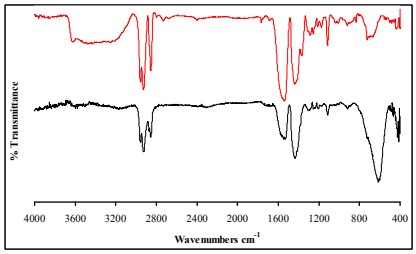

Figure 2: IR spectra of nickel-iron (octanoate) precursor (a) as-prepared and (b) after heating in tetralin for 12 h.

The absorption bands at 2855 cm^{-1}, 2926 cm^{-1}, and 2956 cm^{-1} exhibited by the precursor are attributed to the $–CH_3–$ and $–CH_2–$ aliphatic moieties, while the presence of the carboxylate ($–COO^-$) groups is confirmed by two absorptions at 1529 and 1439 cm^{-1}. Observation of these IR bands confirms the anchoring of caprylate anions to the surface of the nanoparticles. The small separation of 90cm^{-1} between the symmetric and asymmetric carboxylate stretches suggests a chelating or both chelating and bridging modes for coordination for the caprylate moieties to the surface. Figure 3 demonstrates the chelating nature of carboxylate coordination, and combinations of chelating and bridging modes of carboxylate-metal coordination.

Octanoate capped nickel ferrite nanoparticles showed the best dispersability in toluene. The average particle size calculated by using DLS data was about 14.1 nm. It is believed that due to limitations associated with the DLS technique such as the tendency of smaller particles to aggregate quickly in solutions resulting in a larger than expected average particle size, a smaller average particle size is expected using TEM. Therefore, for comparative purposes and better accuracy, transmission electron microscopy was used for average particle size determinations.

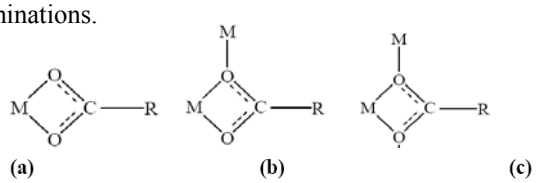

Figure 3: (a) carboxylate ion, RCO_2^-, coordinated to metal (M) as a chelating ligand and in arrangements involving both (b) - chelating and (c) – bridging.

Figure 4 shows the TEM micrographs of octanoate capped (a) and stearte capped (b) nickel ferrite nanoparticles. Spherical particles of somewhat uniform size distribution are observed for (a). An average particle diameter of 5 nm and 11 nm was calculated for (a) and (b) respectively.

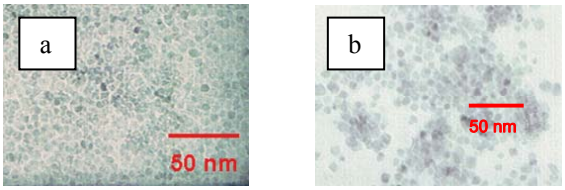

Figure 4: TEM images of capped nickel ferrite nanoparticles (a) octanoate and (b) stearate.

Magnetic properties measurement shows that synthesized nanoparticles were superparamagnetic with zero coercivity, leading to conclusion that the particles size were less than single-domain state. Magnetic hysteresis loop of the sample is shown in Figure 5. The magnetization of 42.5 emu/cc achieved at 10^4 Oe, however, maximum saturation its not conquered in that magnetic field.

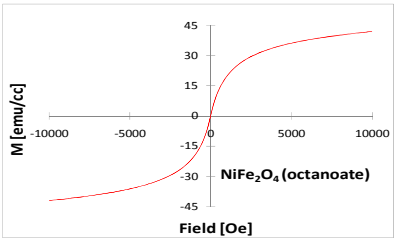

Figure 5: Hysteresis loops of $NiFe_2O_4$ (octanoate) nanoparticles.

Adsorption experiments and detection method: 100 ml glass bottles used for the sorption reactions were cleaned with 10% nitric acid, and washed several times with de-ionized water. 100 ml aliquots of arsenate concentrations ranging from 800 µg/l to 2000 µg/l were treated with 0.1 g of the nanoparticle samples. The mixtures were shaken on a rotor at about 70 rpm for 5 hours. After equilibrium, the final concentrations were detected using the QUICK™ (481396) Arsenic kit. In this detection method, tartaric acid and zinc dust are reacted with the treated solution for the reduction of arsenic compounds to arsine gas. The generated arsine

gas is then allowed to react with a mercuric bromide testing pad. The intensity of the color obtained is proportionately related to the concentration of arsenic in the sample and was determined using a standardized color chart. The reduction reactions are described as follows:

$$5\ H_2AsO_4^{-1} + 20\ Zn + 45\ H^+ \longrightarrow 5\ AsH_3(g) + 20\ Zn^{+2} + 20\ H_2O$$

Generally, van der Waals force, electrostatic forces, exchange of ions, and the lyophobic nature of the adsorbate are the main factors involved in the adsorption process. In all the experiments presented in this study, the uptake of arsenate by the extractants is assumed to be an outcome of chemical coordination or physical attraction between the arsenate and the surface of the adsorbent. Therefore, the maximum number of surface adsorption sites must be finite. The dynamic equilibrium established between the adsorbate concentrations on the adsorbent surface and in solution at a constant temperature is expressed by the linearized Langmuir adsorption isotherm. The shape of the adsorption isotherms can be approximated by the Langmuir equation generally expressed as:

$$X = \frac{\theta^o K C_{eq}}{1 + K C_{eq}} \quad (1).$$

Where **X** is the amount of As(V) adsorbed per unit weight of adsorbent (mg/g), It can also be referred as the adsorption density at the equilibrium solute concentration (C_{eq}), $\mathbf{C_{eq}}$ is the equilibrium concentration of As(V) in aqueous solutions (mg/l), $\boldsymbol{\theta^o}$ (mg/g) is the maximum adsorption capacity corresponding to the complete adsorbate coverage of an adsorbent monolayer, and it's one of Langmuir constants, **K** (l/mg) is the Langmuir constant related to the energy of adsorption by an Arrhenius-type equation expressed in the form: $K = K_o e^{\frac{-E}{RT}}$. Where $\mathbf{K_o}$ is a constant containing the entropy, **E** is the adsorption energy, **R** is the universal gas constant, and **T** is the absolute temperature. The rearrangement of Eq 1 gives the following linear form: $\frac{C_{eq}}{X} = \frac{C_{eq}}{\theta^o} + \frac{1}{\theta^o K}$. A linear plot of C_{eq}/X versus C_{eq} using this equation implies that the Langmuir model fits the generated data. It has been found that the adsorbents developed and used for this specific application were superior to other adsorbents used for arsenic removal such as activated charcoal, hydrous ferric oxide, and zero valent iron [11]. At pH 6, all adsorbents in this study were able to reduce arsenate levels in solutions below new EPA standards (10 µg/l). Figure 6 shows the As(V) adsorption data fitted with the Langmuir model where good coefficients of determinations (R^2) were determined for the three adsorbents.

4 CONCLUSIONS

Carboxylate capped magnetic nanoparticles were synthesized under anaerobic conditions using a novel non-hydrolytic approach. The prepared nanoparticles exhibited unique properties such as structural uniformity and small size. Their magnetic activity allows for future utilization in many environmental and biological applications such as HGMS of arcenic contamination in the water.

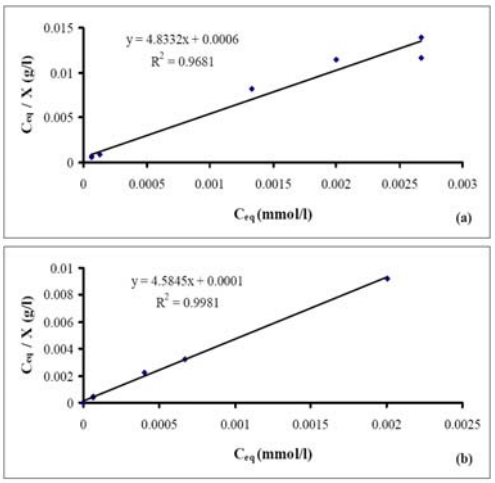

Figure 6: Langmuir isotherms for the adsorption of As(V) from aqueous solutions using (a)- octanoate and (b) stearate capped nanoparticles.

ACKNOWLEDGMENTS

We wish to acknowledge the financial support of this research by the National Science Foundation, grant # 0933140.

References

[1] T.V. Nguyen, S. Vigneswaran, H.H. Ngo, D. Pokhrel, T. Viraraghavan, Eng in Life Sci, 6, 86, 2006.

[2] S.L. Chen, S.R. Dzeng, M.H. Yang, K.H. Chiu, G.M. Shieh, C.M. Wai, Env. Sci and Tech, 28, 877, 1994.

[3] O.S. Thirunavukkarasu, T. Viraraghavan, K.S. Subramanian, Water Quality Research Journal of Canada 36, 55, 2001.

[4] R.P. Kumar, S. Chaudhari, K.C. Khilar, S.P. Mahajan, Chemosphere, 55, 1245, 2004.

[5] United States. EPA. Office of Water.; Washington, DC, 2002.

[6] A. Zouboulis, I. Katsoyiannis, Sep Sci and Tech 37, 2859, 2002.

[7] United States. EPA. Office of Solid Waste and Emergency Response. Arsenic treatment technologies for soil, waste, and water: Washington, D.C., 2002.

[8] G.D. Moeser, K.A. Roach, W.H. Green, P.E. Laibinis, T.A. Hatton, Ind & Eng Chem Res, 41, 4739, 2002.

[9] J. Rockenberger, E.C. Scher, A.P. Alivisatos, J. Amer Chem Soc, 121, 49, 11595, 1999.

[10] X.M. Liu, S.Y. Fu, C.J. Huang, *J. of Magn. Magn. Mater, 281* (2-3), 234, 2004.

[11] S. Kundu, A. Pal, M. Mandal, S.K. Ghosh, S. Panigrahi, T. Pal, *J. Env Sci and Health, Part A: Toxic/Hazardous Substances & Environmental Engineering A39*, 185, 2004.